ISSN 1069-3513, Izvestiya, Physics of the Solid Earth, 2006, Vol. 42, No. 1, pp. 27–40. © Pleiades Publishing, Inc., 2006.
Original Russian Text © S.S. Arefiev, E.A. Rogozhin, V.V. Bykova, C. Dorbath, 2006, published in Fizika Zemli, 2006, No. 1, pp. 30–44.

Deep Structure of the Racha Earthquake Source Zone from Seismic Tomography Data

S. S. Arefiev*, E. A. Rogozhin*, V. V. Bykova*, and C. Dorbath**

**Schmidt Institute of Physics of the Earth, Russian Academy of Sciences, Bol'shaya Gruzinskaya ul. 10, Moscow, 123995 Russia*

***Institut de Recherche pour le Dévelopment, École et Observatoire des Sciences de la Terre, Strasbourg, France*

Received July 27, 2004

Abstract—The Racha earthquake of 1991 was the strongest of the earthquakes recorded in the Caucasus. It was studied by an international epicentral expedition. Unique data gathered by this expedition included records of aftershocks whose swarm was very intense. A 3-D velocity model is obtained from analysis of these data by the method of local earthquake tomography. The ancient crystalline basement and the sedimentary–volcanic Mesozoic–Cenozoic cover could be identified from cross sections of the *P* wave field. The eastern and western boundaries of an uplift in the basement of the Dzirulskii Massif are delineated. Linear low velocity heterogeneities correlating with the active Kakheti-Lechkhumi fault zone and two Trans-Caucasian linear fault zones are discovered in the basement. The cloud of aftershock hypocenters is shown to correlate with a reflector coinciding with the cover–basement interface.

PACS numbers: 91.30Px

DOI: 10.1134/S1069351306010034

1. INTRODUCTION

The Racha, April 29, 1991, earthquake was the strongest of the earthquakes recorded in the Caucasus. Its magnitude, $M_W = 7.0$ (CMT) or $M_S = 6.9$ (ISC), was the highest in the recorded history of this Caucasian region. The earthquake was studied by an international epicentral expedition, and the catalog of recorded aftershocks included 3792 events [Arefiev *et al.*, 1993]. An important feature of the Racha earthquake was an anomalously low intensity of tremors as compared with its high magnitude and the small depth of its source. The intensity nowhere exceeded 8 and the most severe damage was primarily due to poor quality of construction, weak grounds, and so on. Extensive development of catastrophic slope processes (rockfalls and landslides) was one of the main factors responsible for material and human losses. The earthquake area is very prone to natural disasters even unrelated to earthquakes. This is why even weak tremors of the earthquake initiated ubiquitous slope processes [Rogozhin *et al.*, 1993]. In the eastern and central parts of the source area, some landslides involved water-bearing rocks, which caused the formation of mudflows. One of such mudflows destroyed the village of Khokhety, where casualties were most numerous. The earthquake was also distinguished by a large number of aftershocks of significant amplitudes. The strongest occurred on April 29 (18:30) and June 15 (00:59); the first had the magnitude $M = 6.1$ and the second had the magnitudes $M = 6.2$ [Gabsatarova *et al.*, 1992] and $M_W = 6.3$ (CMT).

Since information on historical earthquakes near the Racha source is absent, one may suppose that the recurrence interval of such earthquakes exceeds 1000 yr. Actually, the Spitak earthquake showed that the strongest Caucasian earthquakes can have very long recurrence intervals [Rogozhin *et al.*, 1990; Philip *et al.*, 1992]. However, the trench method could not be used for the verification of this hypothesis in the case of the Racha earthquake.

Although the Racha earthquake was the strongest event recorded in the Caucasus, historical documents yield no evidence that an earthquake of a comparable energy occurred in the close vicinity of the Racha source. Various methods showed that the mechanism of the main shock was NW-striking (300°) reversed faulting on a gently sloping (35°) plane. This mechanism is well consistent with a ground motion intensity anomalously low for such a magnitude and with geological notions according to which one of the main tendencies of the geological development of the Greater Caucasus is the thrust of the Georgian block basement under the Main Caucasian Range and Flysch anticlinoria. Thus, the Racha earthquake is one of the first well studied and comprehensively described seismic events related to nappe tectonics.

2. TECTONIC POSITION OF THE SOURCE AND COSEISMIC DEFORMATIONS

The tectonic scheme of the Caucasus showing the main features of the basic tectonic process (collision) in the region is presented in Fig. 1. This scheme is widely

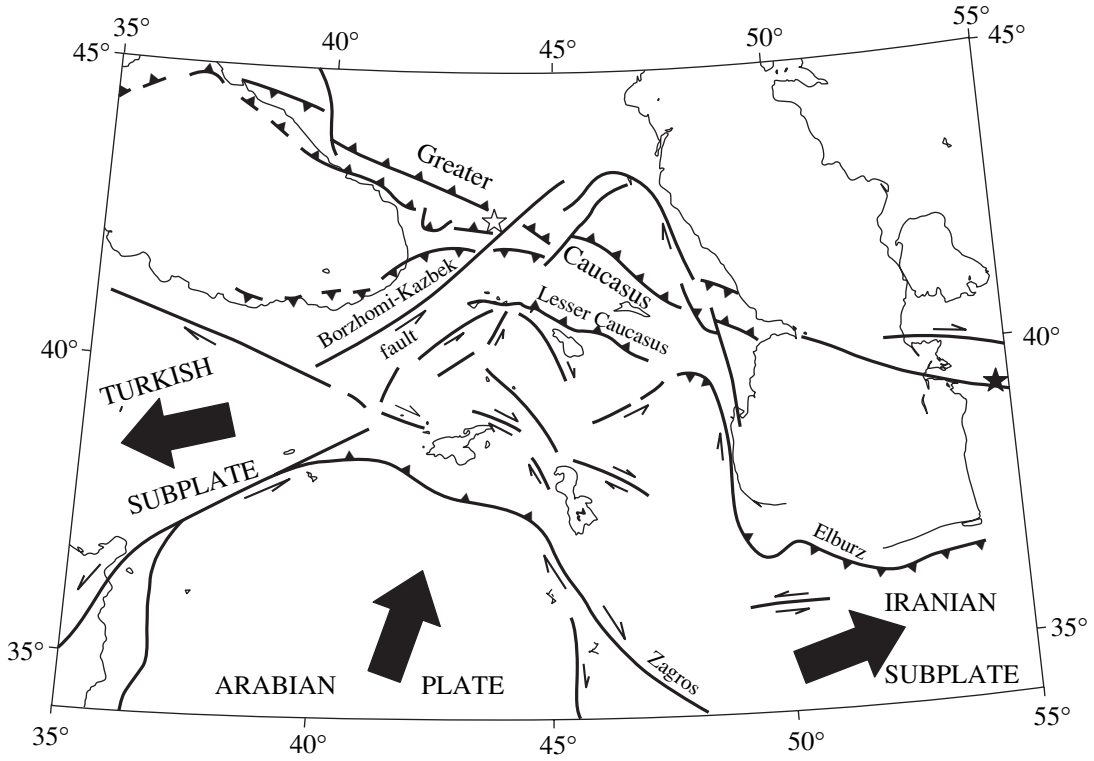

Fig. 1. Tectonic position of the source on a regional scale.

cited, although some authors using it introduce their own, not always justified, corrections. The seismotectonic process is primarily controlled by the northward motion of the Arabian plate relative to the Eurasian plate. Data on motions of plates near their continental boundaries are much more uncertain than at oceanic plate boundaries. The plate interaction at continental boundaries cannot be described in terms of a contact between two solid bodies. Here, it is often impossible to delineate a distinct boundary well expressed in various geological and geophysical fields, as well as in the seismicity pattern. The contact is represented by a boundary zone, sometimes a few hundred kilometers in size. The plates themselves are broken into subplates interacting with each other in an intricate way. However, the main characteristics are controlled by global plate motions; in our case, this is the convergence of the Eurasian and Arabian plates at a velocity of about 3 cm/yr.

Figure 1 clearly displays the overall wedgelike structure of the Caucasus, divided into the smaller Daghestan and Talesh wedges. Thus, the eastern margin of the Racha source zone lies in the intersection area of the Borzhomi-Kazbek fault and the Main Caucasian Range. Both structures have a high rank. The first is traceable up to the North Anatolian fault, and the second crosses the Caucasus from the Caspian Sea to the Black Sea and extends to the west (and possibly to the east). This region is geologically well studied (e.g., see [Milanovsky and Khain, 1963; Milanovsky, 1968; Gamkrealidze and Gamkrealidze, 1977; Maisuradze and Lebedeva, 1979; Bogachkin *et al.*, 1992; Philip *et al.*, 1989]). The main feature of the earthquake area is the thrust of the Georgian block (the Dzirulskii Massif) under the Main Caucasian Range. West of the Borzhomi-Kazbek fault, this underthrust has a tectonic nappe form (Fig. 1). Main reverse faults are represented by gently sloping surfaces under a sedimentary layer that is in turn disturbed by folding, faults, and fractures. All this makes the Greater Caucasus similar to a bulldozer pushing the sedimentary cover to the south and crushing the basement.

Experimental observations including geological studies have not revealed traces of the source rupture on the Earth's surface, but secondary manifestations of the earthquake such as landslides, ruptures associated with the landslides, and so on were numerous and diverse [Borisov and Rogozhin, 1993; Gibson *et al.*, 1993; Rogozhin *et al.*, 1993].

The near-field area of the Racha earthquake, i.e., the territory of the strongest effect of seismic vibrations, includes the vast majority of aftershock epicenters and nearly all coseismic deformations of the ground [Gibson *et al.*, 1993] (Fig. 2). This area is bounded by well-known geological structures: in the east, by the Tskhinvali-Kazbek deep fault, whose seismotectonic significance has been proven by many researchers [Bogachkin and Rogozhin, 1993; Milanovsky and Khain, 1963; Adamiya *et al.*, 1989; Milanovsky, 1968; Borisov

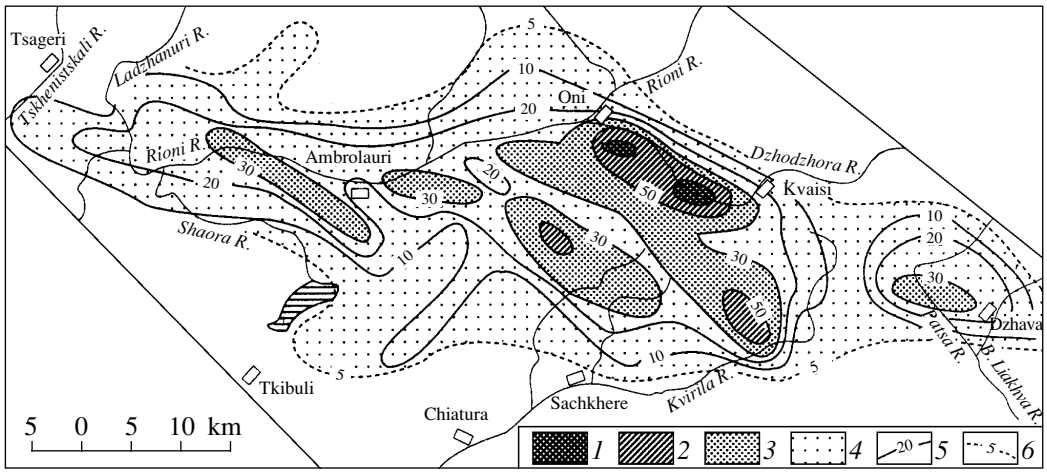

Fig. 2. Map showing the distribution density of coseismic deformations in the Racha earthquake area: (*1–4*) number of deformations per unit area (5 × 5 km): (*1*) >70, (*2*) 50–70, (*3*) 30–50, and (*4*) 5–30; (*5*) distribution density contours of coseismic deformations; (*6*) contour delineating the field of deformations.

et al., 1975; Gamkrealidze and Gamkrealidze, 1977]; in the south, by the boundary between the Okrib–Sachkhere zone and the Dzirulskii Massif; in the west, by the transverse Rioni-Kazbek fault [Bogachkin and Rogozhin, 1993], separating the Svanetsko-Sorskii anticlinorium from the eastern pericline of the Gagra–Dzhava zone; and in the north, by the Orkhibsko-Utserskii upthrow–thrust, bounding here the Flysch synclinorium to the south. According to the distribution of coseismic surface deformations and epicenters of aftershocks, the Racha earthquake source was confined to the Racha–Lechkumi segment of the Kakheti-Lechkhumi suture zone. Being the largest tectonic disturbance of the southern slope of the Greater Caucasus, the Kakheti-Lechkhumi suture zone separates the Dzirulskii inlier of the median mass of the Georgian block from the fold zone of the southern slope of the Greater Caucasus. Although the source faulting plane does not coincide with the plane of this large fault zone, there are no doubts that the latter is structurally associated with the source itself.

Numerous surface deformations arose in the near-field zone during the earthquake and some time after its main shock. They were all of secondary nature and were due to seismogravitational and (in part) vibratory effects. Primary seismotectonic deformations directly reflecting the faulting in the source occurred nowhere.

Seismogravitational fractures (consequences of a catastrophic acceleration of slope processes) are subdivided into the following types (in decreasing order of their occurrence): rockfalls and talus slides, slope detachments (embryonic décollements), rock and rock–earth avalanches, clayey landslides, and block (structural) slides. Deformation types in a specific area are determined by ground conditions, topographic patterns, bedrock lithology, and the geological structure [Gibson *et al.*, 1993].

Rockfalls in the epicentral zone took place on nearly all truncated or gullied slopes, cuesta scarps, and so on. The most significant deformations of this type, involving volumes of up to 0.1 km^3, are confined to steep cliffs of the Racha Ridge composed of Cretaceous limestones and to valley slopes of the Dzhodzhora River near the village of Iri; they were also developed in the upper parts of the Kvirila and Chikhura rivers, where surface beds are composed of Bajocian volcanics of the Middle Cretaceous. Less significant rockfalls associated with the main shock or the strongest aftershocks were observed in the Rioni, Dzhodzhora, Bolshaya Liakhva, and Patsa river basins, mainly on steep slopes composed of weathered rocks of the Mesozoic and Cenozoic.

The next most frequent coseismic fractures were landslides. There is a clear distinction between clayey landslides of deluvial slopes, particularly in areas where their soles consist of Maikopian (Oligocene–Miocene) gypsum-bearing clays and sandstones, and structural block slides (detachments) involving not only the soil cover and loose ground but also bedrocks (generally limestones and marls) that preserved their geological structure in the process of the deformation.

According to reports of local inhabitants, clayey landslides arose two or three days after the main shock (the shock itself gave rise only to thin embryonic fractures). Slope areas involved in these landslides were characterized by a higher water content and low angles (5°–10°). Such a landslide observed near the village of Chordi was about 0.5 km wide and about 1 km long and had a volume of the order of (15–25) × 10^6 m^3. According to witnesses, the seismic shock did not produce an appreciable ground slip, whereas an active motion (at a velocity of 8 m/day) started later and resulted in the total destruction of the village. Three weeks after the main shock, the landslide was still moving at a velocity of 2–3 m/day.

Landslides of a different type developed on steep (20°–30°) structural slopes composed of nearly dry rocks. Thus, a landslide between the villages of Usholta and Shkmeri affected not only the diluvium but also carbonate bedrocks of the Upper Cretaceous. Ruptures of this type are likely to have occurred immediately during the earthquake. The volume of the detached rock mass reached 2×10^6 m^3.

Rock and mud-rock avalanches are the most grandiose and impressive coseismic deformation features. They were mainly observed in the central (including the instrumental epicenter) and eastern parts of the near-field zone, mostly in South Ossetia. Thus, in the upper part of the Kvirila River basin, a huge rock mass about 30×10^6 m^3 in volume (Bajocian volcanics of the Middle Jurassic) broke off and fell from a height of about 300 m onto water-saturated alluvial deposits of the Khokhietistskali River flood plain and uplifted terraces. The latter played the role of a lubricant at the sole of the sliding rock mass, so that a rockfall was transformed into a rock avalanche that traveled in the horizontal direction for more than one kilometer along the Khokhietistskali River valley and entered the larger valley of the Gebura River, destroying the village of Khokheti and killing its inhabitants. A branch of the avalanche was upthrown onto the opposite slope of the Khokhietistskali River valley, reaching a height of more than 100 m. The avalanche dammed the river, forming a system of ponds. Similar, although less significant, rock and mud-rock avalanches descended from steep slopes and dammed the rivers Kvedrula (in its upper stream), Kvirila (in the area of the village of Tbeti), and Patsa (near the settlement of Dzhava).

Surface ruptures in the form of seismogenic fractures unrelated to gravitational phenomena are comparatively rare. Such deformations on the crest of the Khikhata Ridge (the southern branch of the Racha Ridge) form a system of subparallel, occasionally en echelon arranged, WNW-trending tension fractures 1.5 km in overall length. Large limestone blocks "thrown" for tens of meters were also observed here [Gibson *et al.*, 1993]. This phenomenon indicates that local vertical accelerations here exceeded 1 *g*.

Coseismic deformation features were distributed nonuniformly in the area 70×30 km^2 in size bounded by the longitudes of the village of Khvanchkara and the settlement of Dzhava and by the latitudes of the towns of Oni and Sachkhere (this territory generally coincides with the area of the aftershock cloud and apparently with the projection of the main shock source zone onto the Earth's surface).

Interpretation of satellite and aerial photographs taken before and after the earthquake was used for mapping numerous deformation features, and statistical treatment of data on their areal distribution and the contour interpretation of its results revealed a regular pattern of these heterogeneities [Bogachkin *et al.*, 1993]. A general inspection of higher concentration areas of residual deformations within the field of coseismic disturbances shows that they can be united into two separate zones: a northern zone bounding the source area to the north and a southern slightly arcuate zone bounding the source to the south.

A special study showed that the inhomogeneous distribution of secondary coseismic disturbances in the near-field zone does not correlate with topography and geological–geomorphological structure, implying that this inhomogeneity was due to a deep-seated factor, namely, the structure of the seismic source. Therefore, the secondary coseismic disturbances on the surface indirectly reflect the source structure [Rogozhin *et al.*, 1993; Bogachkin *et al.*, 1993].

Comparison of the distribution of secondary surface deformations with the field of aftershock epicenters revealed a remarkable correlation between geological features and seismological manifestations in the central part of the source area [Rogozhin *et al.*, 1993; Bogachkin *et al.*, 1993]. This confirms our suggestion that concentration areas of residual deformations delineate the surface projection of the deep-seated source of the earthquake.

Apparently, the late Alpine thrusting of the crystalline basement of the Georgian block under the southern slope of the Greater Caucasus reconstructed in [Adamiya *et al.*, 1989; Gamkrealidze and Gamkrealidze, 1977] was the mechanism that triggered the Racha earthquake. In the sedimentary cover of tectonic zones of the southern slope, thick strata of the flysch synclinorium are thrust over the sedimentary complex of the Gagra–Dzhava zone, and the latter is in turn thrust over the sedimentary–volcanic cover of the Okrib–Sachkhere zone. Clays and shales of the Alpine cover base, as well as other ductile beds, form zones of a lower sliding friction facilitating the development of subhorizontal slips.

3. LOCAL EARTHQUAKE TOMOGRAPHY

For the tomographic analysis, we utilized the SIMULPS12 program [Evans *et al.*, 1994] using V_p and V_p/V_s (initially *S*–*P*). Experimental data were obtained from epicentral observations of 1991 in the Racha earthquake zone. The observations were conducted at 52 network stations over the period from May 8 to August 22, 1991. Only 45 of the stations yielded more than 100 phases. Initial positions of hypocenters were determined with the help of the HYPO71 program [Lee and Lahr, 1975]. Of the whole data set (more than 3000 events), we selected events for which no less than 7 phases (including no less than 2 *S* phases) were available and rms errors of hypocentral solutions did not exceed 0.30. These criteria were met by 1323 events, which yielded 12 745 *P* and 8274 *S* traveltimes.

In accordance with the method of local earthquake tomography, the study area was divided into a three-dimensional $20 \times 14 \times 8$ grid whose surface projection

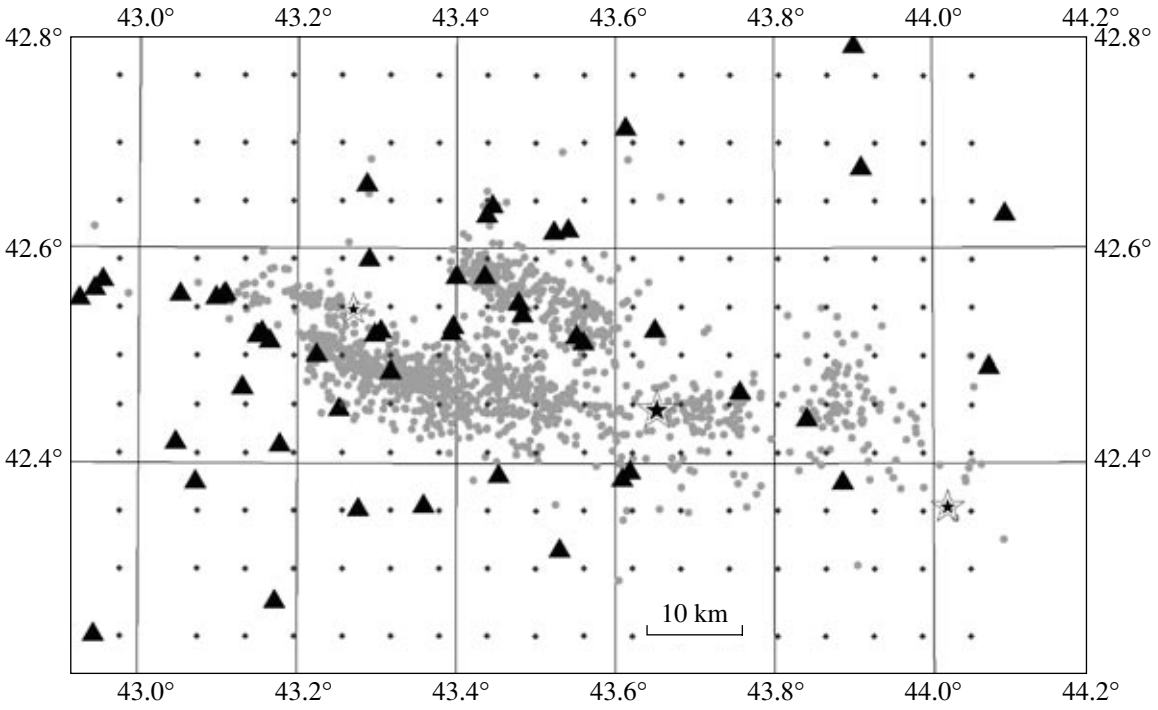

Fig. 3. Studied area: triangles are seismic stations, dots are grid nodes, shaded circles are aftershock epicenters, and stars are the main shock and the strongest aftershocks.

is shown in Fig. 3. Edge nodes of the grid are not shown because, in accordance with the requirements of the method, they are far beyond the area studied. Figure 3 also shows the recording stations and epicenters of earthquakes. The method admits the use of an irregular grid. Therefore we chose the following partitioning expressed in kilometers relative to the center of the study area (42.5°N, 43.5°E): –700.0, –43.0, –35.0, –30.0, –25.0, –20.0, –15.0, –10.0, –5.0, 0.0, 5.0, 10.0, 15.0, 20.0, 25.0, 30.0, 35.0, 40.0, 45.0, and 700.0 along latitude; and –700.0, –55.0, –29.0, –22.0, –16.0, –10.0, –5.0, 0.0, 5.0, 10.0, 16.0, 22.0, 29.0, and 700.0 along longitude. The following depth levels were chosen: –3.0, 0.0, 3.0, 6.0, 9.0, 12.0, 20.0, and 40.0 km. We should note that some levels and cross sections were represented by inadequate amounts of data. For this reason, we constructed additional maps of the resolution parameter (that are not presented here) for each level and cross section. In accordance with these maps, velocity values are shown as shades of gray only in those areas of the study region where the resolution was no worse than 0.1. Velocity contours were constructed in the entire region.

The damping parameter is important in calculations by the method of Thurber [1983]. We estimated this parameter empirically by a method similar to that proposed by Eberhart-Phillips [1986] and set it equal to 30. The *P* velocity model calculated in this way is shown in Figs. 4–7.

As mentioned above, the aftershock sequence of the Racha earthquake was fairly intense. The strongest (M_W = 6.3) aftershock, known as the Dzhava earthquake, occurred at the western end of the source zone on June 15, 1991, 1.5 months after the main shock (M_W = 7.0). The quality and volume of data allowed us to perform additional analysis, dividing the time period under consideration into two time intervals, before and after this aftershock. These intervals included 551 and 772 events, respectively. However, the eastern part of the source zone was represented by fewer data (a smaller number of earthquakes suitable for the filter described above), although the complete map of epicenters (more than 3000 events) displays a cluster in this area. In particular, this was the reason why the resolution of cross section G in the eastern part of the zone was below the chosen threshold and a shaded area is absent here. A greater amount of data was available for the central and western parts of the source zone in the time interval following the strongest aftershock, so that the related results are better controlled compared to the interval preceding the aftershock.

4. TECTONIC INTERPRETATION OF EARTHQUAKE TOMOGRAPHY RESULTS

Tomographic slices obtained in the earthquake source zone at various depths (Fig. 4) are usable for tracing structural heterogeneities from the Earth's surface to a depth of 12 km. A general increase in the *P* wave velocity with depth is observed. In surface layers (0–3 km), the *P* velocity ranges predominantly from 3.5 to 5.5 km/s. The only significant variations in the velocities in this depth interval are lateral. Thus, the

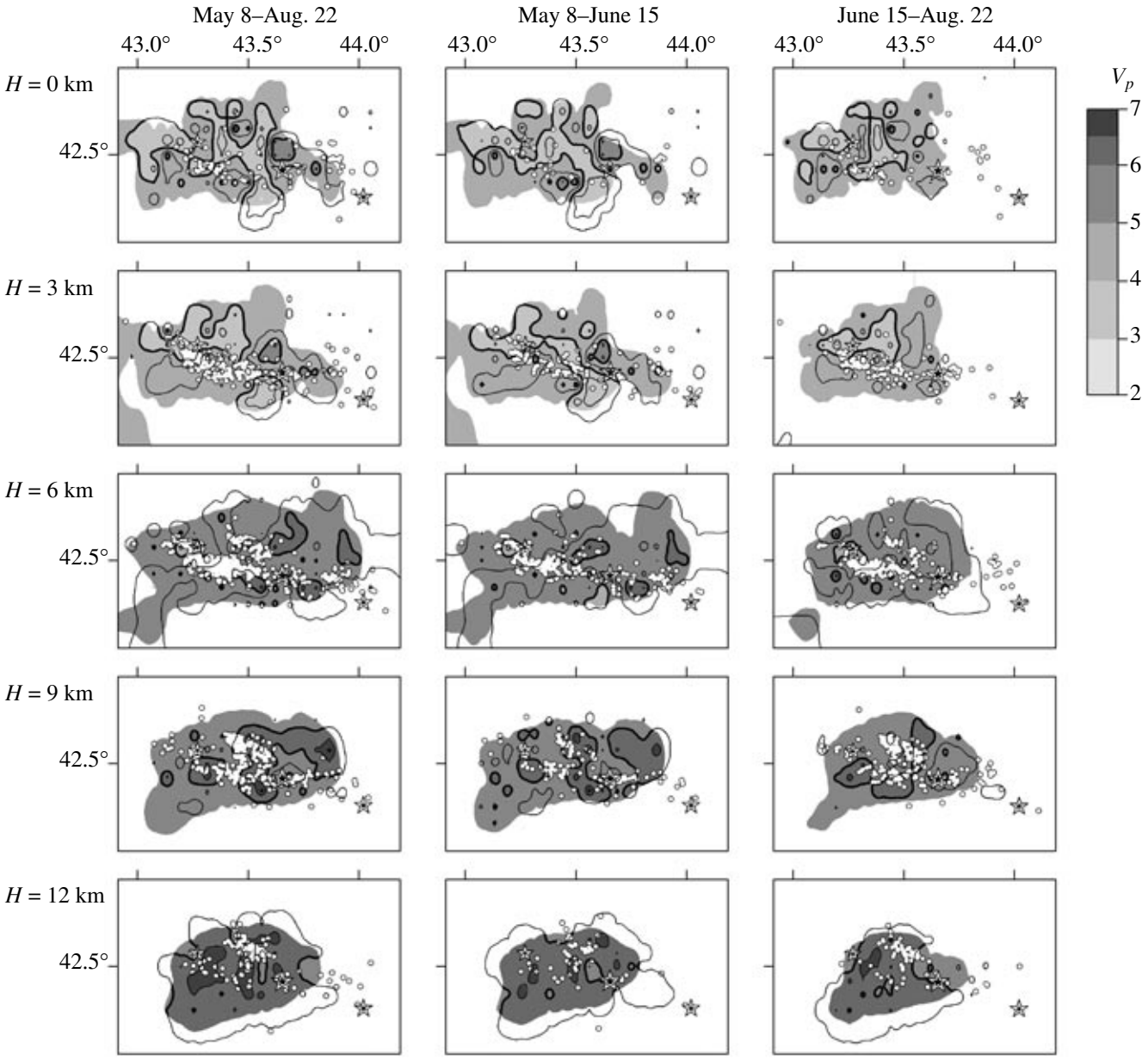

Fig. 4. Horizontal cross sections of the *P* wave velocity field shown for various time intervals. The shaded areas were obtained at a resolution of no worse than 0.1. Each map shows earthquakes whose depths lie within the corresponding layer. The large stars are the main shock and the strongest aftershocks.

velocities are generally lower in the northern part of the source zone (3.5–4.5 km/s) and are higher in the southern part (4.5–5.5 km/s). This distribution of velocity heterogeneities is virtually invariable in the upper (at a depth of 0 km) and the lower (3 km) parts of the section. In addition to this general E–W zonality (consistent with the Caucasian orientation), smaller heterogeneities having the N–S (Trans-Caucasian) orientation are clearly observed here. They are represented by two bands of higher velocities (4.5–5.5 km/s) alternating with bands of lower (3.5–4.5 km/s) V_p values. The lower and higher velocity bands are 5–10 km wide.

It is noteworthy that the compact southern part of the cloud of aftershock hypocenters gravitates toward the higher velocity zone in the upper part of the section, whereas no aftershocks are observed at these hypocentral depths in the higher velocity northern zone.

The velocity pattern changes dramatically at depths of 6 and 9 km (Fig. 4). The *P* wave velocity in this range of depths varies laterally from 5 to 7 km. Here, in the southern and northern parts of the source zone (respectively, in the southern and northern areas of concentration of aftershock hypocenters), two narrow (10–20 km) 70–80-km long WNW-striking bands of higher V_p values

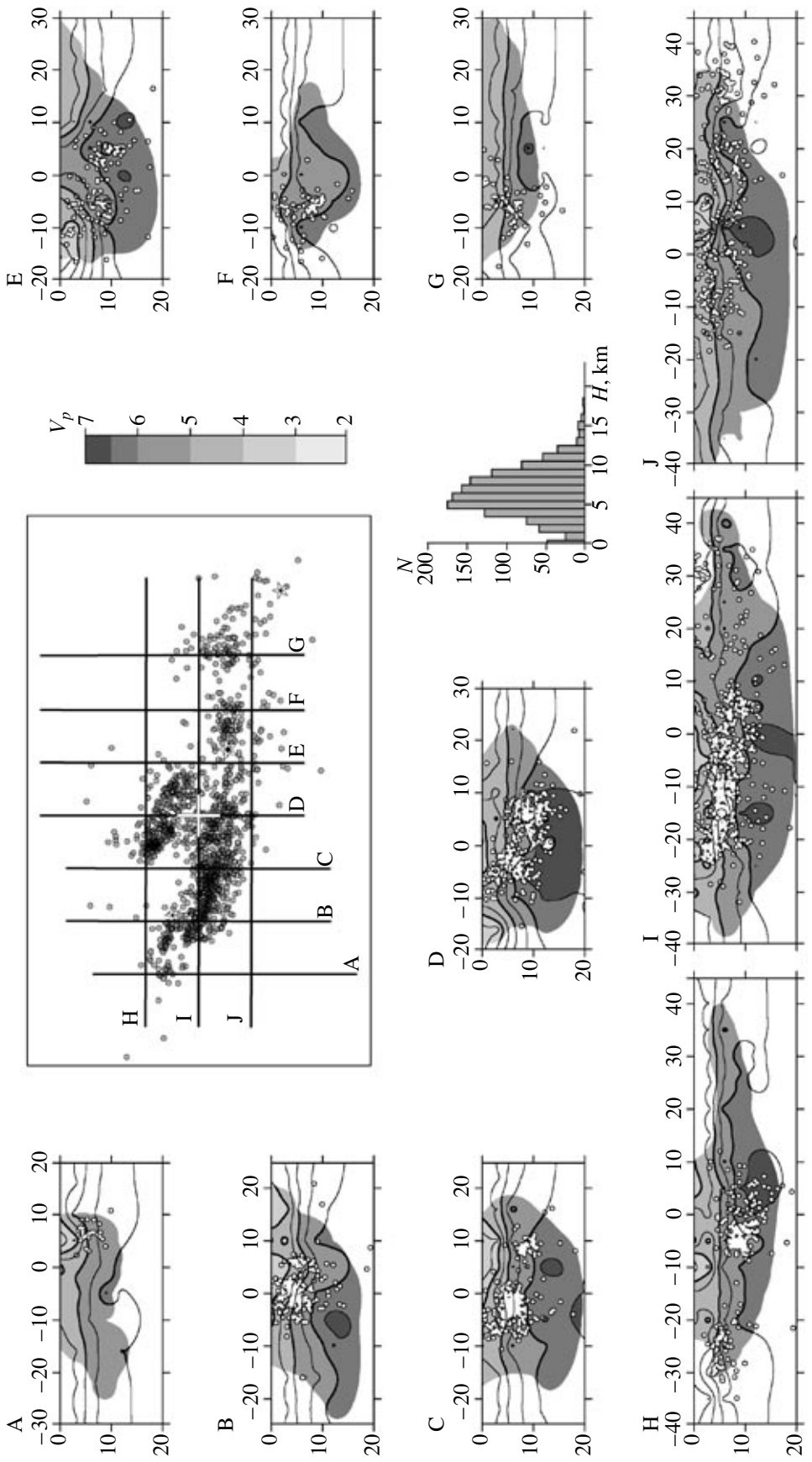

Fig. 5. Vertical cross sections calculated for the entire time interval along profiles shown in the middle upper panel, where the open cross fixes the origin of coordinates used in the calculations. The shaded areas were obtained at a resolution of no worse than 0.1. The histogram shows the depth distribution.

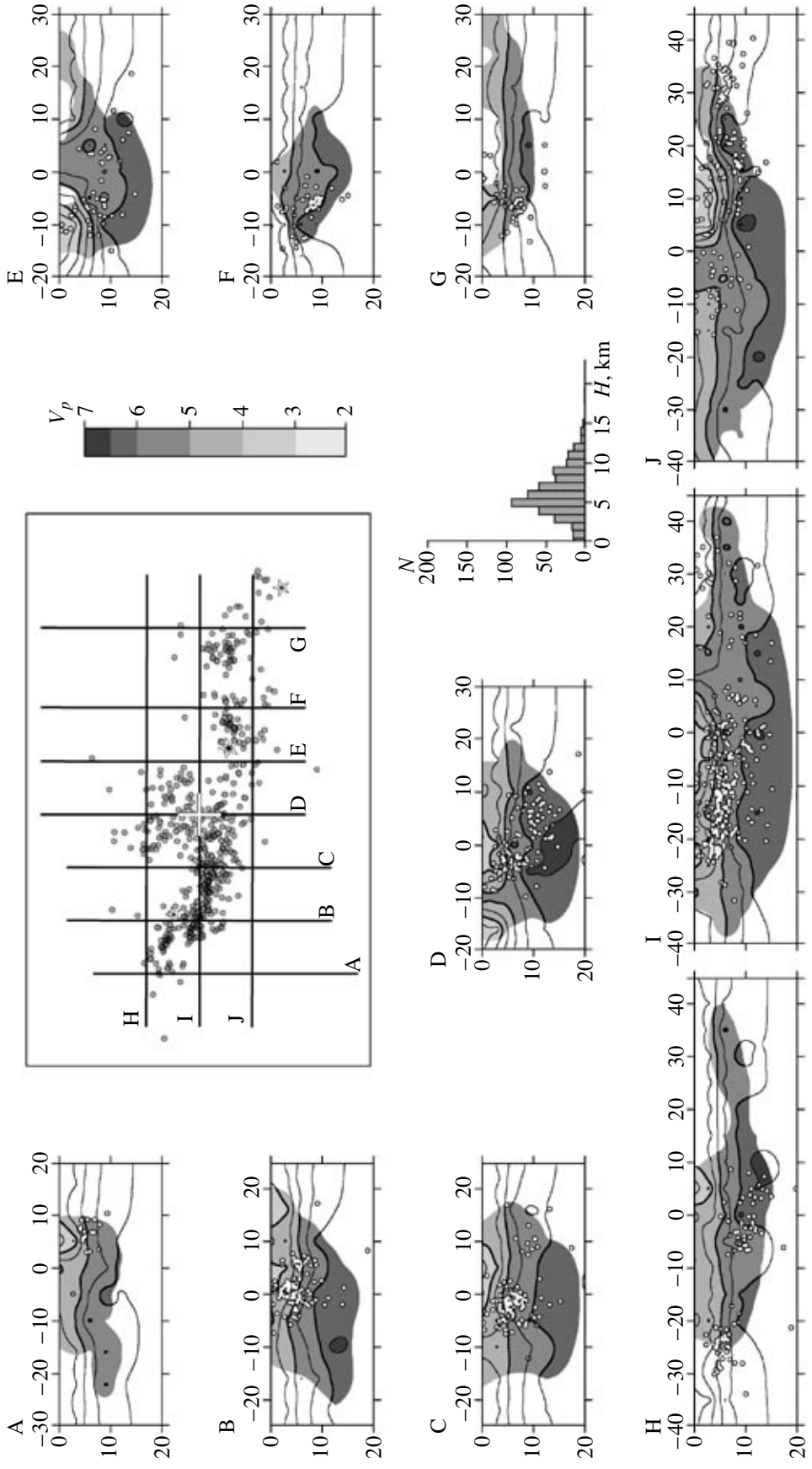

Fig. 6. Vertical cross sections calculated for the time interval preceding the strongest aftershock. The rest of the notation is the same as in Fig. 5.

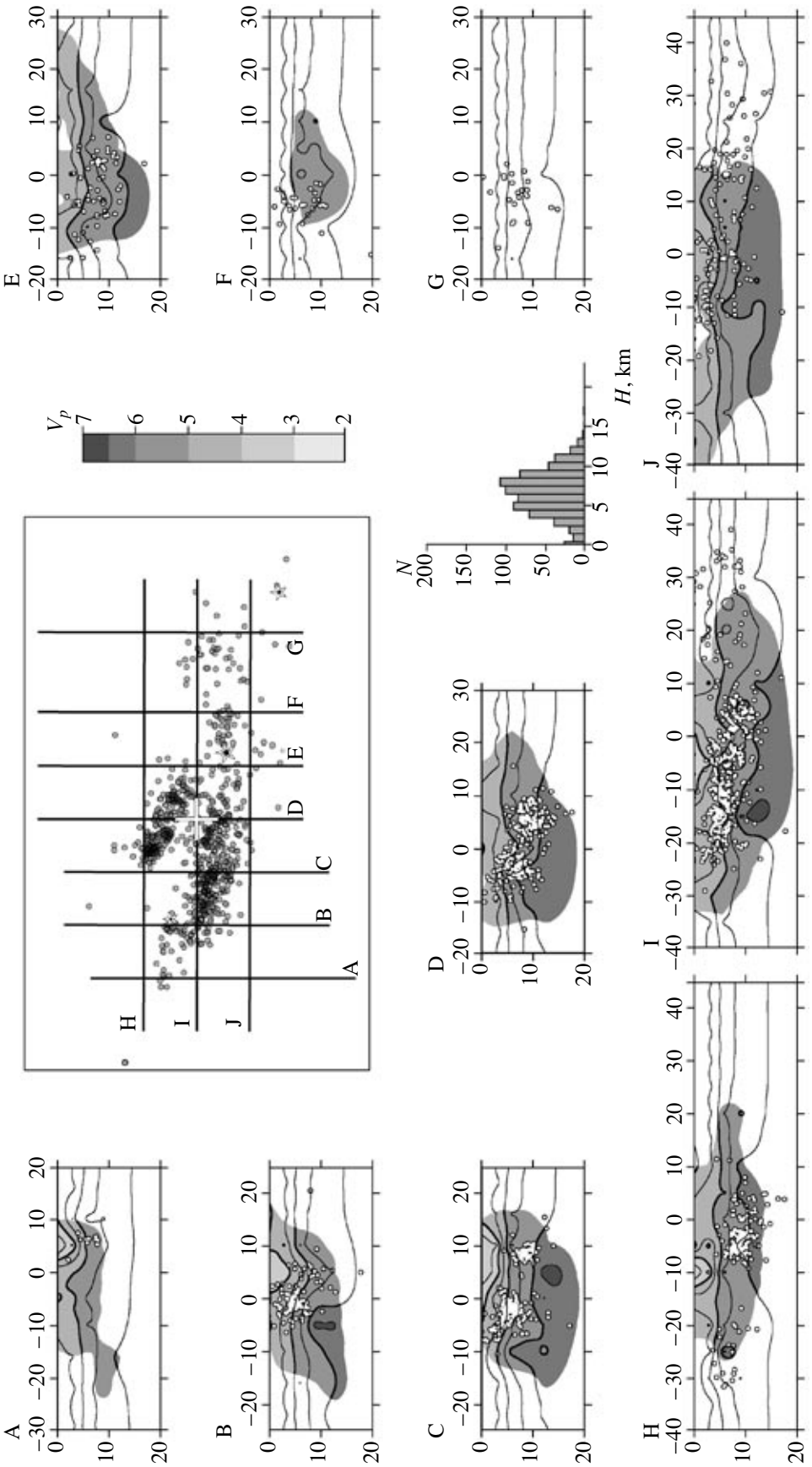

Fig. 7. Vertical cross sections calculated for the time interval following the strongest aftershock. The rest of the notation is the same as in Fig. 5.

(6–7 km/s) are observed; lower velocity areas (5–6 km/s) separate and bound these zones to the north and south. The separating lower velocity band is about 10 km wide. At these depths, the clearly expressed zonality of the Caucasian orientation is virtually undisturbed by linear heterogeneities of the Trans-Caucasian (N–S) orientation.

The 12-km slice displays the prevalence of relatively high *P* velocities (6.5–7 km/s) in the entire area of the source zone. Lower V_p values (5.5–6 km/s) are observed only in small areas in the central and eastern parts of the zone. A lateral heterogeneity represented by a narrow (10 km) band of lower velocity (5.5 km/s) in the middle part of the source zone emphasizes here the Trans-Caucasian (N–S) control.

The following geological interpretation of the observed vertical and lateral heterogeneities can be proposed. The upper 6 km of the section, characterized by low seismic velocities, are composed of sedimentary and volcanic sequences of Mesozoic and Tertiary ages. The northern part of the Racha earthquake source zone is mainly represented by terrigenous–carbonate flysch deposits of the Upper Jurassic and Lower Cretaceous of the Chiatura zone and by Lower–Middle Jurassic arenaceous–shaly flyschoid deposits of the Gagra–Dzhava zone. The Lias thickness is strongly reduced to the south, within the Racha–Lechkhumi and Okrib–Sachkhere structural–facial zones, whereas the bulk of the cover is represented by Bajocian spilite–diabase strata of the Middle Jurassic including small thin caps of Jurassic limestones and Oligocene–Miocene terrigenous beds.

The Bajocian volcanics more than 5 km in thickness developed in the south of the epicentral area are undoubtedly denser and less fractured than the strongly schistose flysch and flyschoid rocks in its north. Accordingly, the velocities in the former rocks are higher. The higher fracturing in the upper parts of the sedimentary cover of the fold system is controlled by the Caucasian structural trend, i.e., the orientation of axes of folds and major faults (in particular, the Kakheti-Lechkhumi zone of deep faults), but also by Trans-Caucasian structures distinctly traceable in this region from remote sounding data [Bogachkin *et al.*, 1993].

The crustal section in the depth interval 6–9 km encompasses the boundary zone of the lower sedimentary horizons and the upper part of the crystalline basement. According to geophysical data, the basement surface, generally dipping at low angles northward under the axial part of the Main Caucasian Range, is irregular and serrate in the meridional cross section. Evidently, these features of the basement surface topography account for the presence of narrow alternating bands of higher and lower velocities in the earthquake source zone. In the 6- and 9-km slices, basement uplifts appear to correlate with high velocity bands and basement depressions, with low velocity bands. It is important to note that dense clusters of aftershock hypocenters are mostly confined to these high velocity uplifts of the basement.

The deepest slice is consistent with the *S* wave velocity distribution pattern in the crystalline basement. The Caucasian zonality of the WNW orientation is poorly recognizable here, whereas the N–S heterogeneity is clearly observable here, apparently, due to two deep faults of the Trans-Caucasian strike in the central part of the source zone, near its eastern and western boundaries.

We should note that the deep velocity distribution patterns are different in the time periods from May 8 to June 15 (when the Dzhava M_W = 6.3 earthquake occurred at the eastern margin of the Racha earthquake zone) and from June 16 up to August 22, 1991, the last day of the local seismic network operation. The distinctions of the latter period are a certain general decrease in *P* wave velocities observed in slices at depths of 6, 9, and 12 km and a nearly complete disappearance of linear features in the distribution of lateral velocity heterogeneities, as is evident from the 6- and 9-km slices. This phenomenon is likely due to a change in the stress–strain state at these depths related to the fact that, by this time, the largest uplifts of the basement were completely destroyed by aftershocks. Apparently, these destroyed uplifts ceased to exist as high velocity structures one and a half months after the main shock.

Seismotomographic images of the source region are somewhat different in the two time intervals of seismological observations of the aftershock process. This result is obtained here for the first time in the practice of seismological observations in a strong earthquake zone. Therefore, as yet we cannot judge the degree of stability of this effect and cannot answer the question of whether it can be revealed in source zones of other strong earthquakes. However, Shchukin *et al.* [1998] suggested that a change in the stress state of deep interiors, for example, in the source zone of a forthcoming earthquake, leads to a change in the seismic velocity distribution in this zone. In our opinion, the aftershock activity of a strong earthquake should also change the stress–strain state of the medium. Consequently, velocity characteristics of layers and, therefore, the velocity structure of the source region should also differ in the initial and final periods of epicentral observations of aftershocks.

The V_p cross sections intersecting the source zone along the longer axis of the source and across the longer axis of the cloud of aftershocks reveal vertical and lateral heterogeneities in the velocity field traceable to depths of 18–19 km and elucidate the relationships between these heterogeneities and hypocenters of aftershocks.

The relationship between the source fault plane (emphasized by clusters of aftershock hypocenters) and upper crust velocity heterogeneities reflecting the struc-

ture of the basement and cover can be traced on three profiles (cross sections H, I, and J in Fig. 5) oriented along the longer axis of the aftershock cloud. As seen from the northernmost section H, a compact cluster of aftershock hypocenters is located at depths of 10–15 km, including a considerable part of the high velocity basement. Only a small number of aftershocks of the upper part of the cloud penetrate into the sedimentary cover (up to depths of 5–7 km). The cover–basement interface lies here at a level of 8–10 km. A narrow pocket of relatively low velocities (V_p = 6.0–6.2 km/s) is well expressed in the middle part of the basement uplift, near its western slope. This pocket is 3–5 km wide and reaches a depth of 18 km. Apparently, this decrease in the velocities of the basement can be associated with an active linear fault of the Trans-Caucasian (N–S) orientation.

The longitudinal cross section I shows that almost the whole compact cloud of aftershock hypocenters lies within the cover of sedimentary–volcanic rocks at depths of 4–11 km above the surface of a high velocity uplift associated with the crystalline basement ($V_p \geq 6.0$). In fact, the seismic source seemingly rests on the surface of this basement uplift and is bounded to the west and east by zones in which the high velocity horizons steeply dip to depths of 15 km (in the west) and 18 km (in the east). The uplifted basement region of high velocity rocks is associated with the Dzirulskii inlier of the Georgian block. Note that the eastern and western slopes of the basement uplift, as well as the well-expressed pocket of lower velocity material in the eastern half of the uplift, are related to the presence of faults of the Trans-Caucasian strike.

Cross section J, reflecting the structure of the source zone in its southern part, shows that the most compact part of the cloud of aftershock hypocenters encompasses nearly the whole thickness of the cover down to the basement surface (depths of 8–10 km) and virtually does not penetrate into the basement itself. The aforementioned low velocity pocket extending across the source strike is also observed in the eastern part of the basement uplift but is not expressed as well as in section I.

In all of the three longitudinal cross sections, the basement–cover interface retains its position at nearly the same depth level, slightly dipping northward, and the aftershock cloud rises southward, shifting from the basement to the sedimentary cover.

The transverse cross sections B and C also show that the hypocenters of aftershocks lie directly above the surface of high velocity horizons of the crystalline basement of the Dzirulskii Massif within the overlying sequence of sedimentary (in the north) and volcanic (in the south) rocks of the Mesozoic cover. On profile C, the cloud of aftershocks, compact on profile B, is divided into two compact clusters separated by a region virtually devoid of aftershocks. On the surface of the high velocity basement, both sections display small uplifts separated by small depressions. These irregularities appear to reflect the serrate shape of the basement surface mentioned above. Areas of the highest concentration of aftershocks (the aforementioned clusters) are confined to these small uplifts.

The depth distribution patterns of velocity heterogeneities are nearly the same on cross section D. Here, two separate clusters of aftershock hypocenters are also confined to small uplifts of high velocity material. However, here not only do they encompass lower velocity strata of the cover (as is seen in sections B and C) but they also extend into the region of high velocity material, i.e., into upper horizons of the crystalline basement. This is related to a rise in the surface of the high velocity material from depths of 8–9 km (sections B and C) to depths of 6–7 km, as is observed in section D. The basement surface also occurs at shallower depths in the more eastern cross sections E, F, and G.

The aftershock hypocenters generally deepen to the north, as is seen in all sections intersecting central parts of the aftershock cloud across the longer axis of the source region. Dense clusters of aftershocks in the north are systematically deeper than those in the southern part of the source zone. On the whole, the cloud of hypocenters encompasses depths of 5–15 km in the north and 0–10 km in the south. This configuration of the aftershock cloud indicates that the faulting plane dipped at a low angle northward in the direction of the tectonic zone of the Main Caucasian Range and the Chiatura flysch zone.

On the whole, the tomographic imagery of the lateral and vertical distribution of deep velocity heterogeneities allows one to adequately interpret not only the structure of the basement surface and overlying horizons of sedimentary and volcanic rocks of the cover but also the spatial position of the main faulting plane in the source of this earthquake, which was the strongest in the history of seismological observations in the Caucasus region. Variations in the lithology of rocks composing the cover can be traced from the position of contrasting inhomogeneities of seismic velocities in the cover, and uplifts, depressions, and benches of the basement surface correlate with tectonic disturbances of the Caucasian and Trans-Caucasian orientations.

As seen from the cross sections reflecting the structure of the source zone before and after the Dzhava earthquake of June 15, 1991 (Figs. 6, 7), the cloud of aftershocks of the main shock of April 29, 1991, retained its general configuration and the main features of the depth distribution of their hypocenters. However, it is noticeable that a certain flattening of basement uplifts of material possessing the highest velocities changes, to an extent, the velocity characteristics of the medium. This flattening of the high velocity basement uplifts is likely due to their destruction over the long

period of aftershocks. In our opinion, this structural transformation is a consequence of the development of the source zone in the first period of the aftershock activity rather than a direct result of the shock of the Dzhava earthquake. On the other hand, the transverse sections B–F, oriented N–S (across the source strike), indicate that a dip in the basement surface filled with material of lower *P* wave velocities observed in the interval before the Dzhava earthquake (Fig. 6) is expressed less distinctly than in the subsequent time interval (Fig. 7). This low velocity pocket in the crystalline basement reflects the position of the Kakheti-Lechkhumi deep fault in the cross section. Apparently, this fault, steeply dipping to the north, was activated in the last period of epicentral observations, which was evidently due to active postseismic horizontal and vertical movements fixed by the local GPS network [Prilepin *et al.*, 1997]; moreover, this activation resulted in the formation of open-joint fissures on the crest of the Khikhata Ridge after the Dzhava event [Belousov and Chichagov, 1993; Rogozhin *et al.*, 1993].

5. DISCUSSION

Three-dimensional tomographic imaging of the distributions of heterogeneities in the source zone of the Racha earthquake provided new insights into the deep geological structure of this zone and the relationships between the faulting plane in the source and major deep structures.

Two main structures of the upper crust clearly distinguished from data of the tomographic analysis are the crystalline basement of the Dzirulskii uplift with the velocities V_p = 6.5–7.5 km/s and the sedimentary–volcanic cover with the velocities 3.0–4.5 km/s in sedimentary strata and 4.5–5.5 km/s in volcanic sequences.

In the entire territory of the source region, the basement–cover interface occurs at approximately the same depth (8–10 km), slightly deepening to the north. Well-expressed benches are discovered in the east and the west of the region, where the basement surface abruptly plunges to depths of 15 km (in the west) and 17–18 km (in the east). These benches in the surface structure of the basement correlate with transverse faults separating the Dzirulskii uplift from the Rioni (in the west) and Kartli (in the east) intermontane troughs. These faults striking NE and bounding the epicentral zone of the Racha earthquake to the west and the east are, respectively, the Rioni-Kazbek and Tskhinvali-Kazbek faults [Rogozhin and Bogachkin, 1993].

The Kakheti-Lechkhumi deep fault, expressed on the surface in the form of the narrow extended Racha-Dzhava linear synclinal depression, is traceable as a narrow extended band of lower seismic velocities. This band having the form of a pocket of low velocity material separates the high velocity basement block into the southern and northern benches bounding the E–W zone of the Kakheti-Lechkhumi fault. In the cover, this fault separates high velocity zones of volcanic and carbonate Mesozoic–Cenozoic rocks in the south from sedimentary terrigenous and flysch low-V_p rocks of the Mesozoic composing the northern part of the source zone.

Lineaments of the Trans-Caucasian strike are well expressed in the *P* velocity field in upper horizons of the cover and in the crystalline basement, being represented by narrow linear bands of lower V_p values. In the crystalline basement, the Trans-Caucasian lineaments form pockets of low velocity material extending to a depth of 18 km. Two transverse linear fault zones are observed in the western and eastern parts of the basement uplift. These zones form an en echelon configuration in the epicentral area. The eastern low velocity heterogeneity is well resolved in the central and southern parts of the source region, and the western one is clearly observed in the western part of the region.

The inhomogeneity of the cloud of aftershocks correlates adequately with vertical and lateral heterogeneities resolved by the seismic tomography data. On the whole, the majority of aftershocks are confined to the interface between high and low velocity horizons of the upper crust that are identified, respectively, with the basement and the cover. Lateral clusters of aftershock hypocenters correlate with uplifts of the high velocity basement. The basement surface is slightly inclined northward, and the cloud of aftershock hypocenters dips more steeply in the same direction. In accordance with these relationships, aftershocks in the southern part of the source region are mostly located in the cover, and those in the northern part are mostly located in the basement.

The lateral distribution of seismic velocity heterogeneities somewhat changed with time. Irregularities of the cover–basement interface that were recorded in the period of epicentral observations preceding the Dzhava earthquake of June 15, 1991, were largely attenuated in the subsequent period. Apparently, this is related to the fact that the basement uplifts were reworked by the aftershock process and, at the end of the period of epicentral observations, ceased to exist as high *P* velocity structures.

Overall, the deep structure of the Racha earthquake source zone as determined from seismic tomography data not only confirmed previous conclusions derived from analysis of geological and geophysical data [Rogozhin *et al.*, 1993; Shengelaya, 1984] but also provided new structural constraints that are important for understanding the origin of the main shock source and the development of the aftershock process.

6. CONCLUSIONS

Based on the tomographic analysis of the 3-D distribution of heterogeneities in the *P* wave velocity field, new data are obtained for the structure and evolution of the Racha earthquake source zone.

Vertical cross sections of the *P* velocity field fixed the ancient crystalline basement and the sedimentary–volcanic Mesozoic–Cenozoic cover. The *P* velocity heterogeneities inferred in the cover correspond to the volcanic and sedimentary zones of the Mesozoic section. The basement uplift of the Dzirulskii Massif is delineated in the west and the east in the field of seismic velocities. Low velocity linear heterogeneities detected in the basement correspond to zones of the active Kakheti-Lechkhumi fault and two Trans-Caucasian linear fault zones.

The position of the cloud of aftershock hypocenters is shown to correlate with a velocity interface coinciding with the cover–basement boundary. The high velocity basement uplifts detected in the first period of seismological epicentral observations in the Racha source zone are found to have been somewhat flattened in the subsequent period of observations following the strong Dzhava earthquake. This may be related to a structural change caused by the aftershock process.

ACKNOWLEDGMENTS

We are grateful to all members of the Epicentral Expedition for their efforts in gathering observational data. Most figures were prepared with the help of the GMT software package. This work was supported by the Russian Foundation for Basic Research, project nos. 02-05-64946 and 02-05-64894.

REFERENCES

1. Sh. A. Adamiya, G. L. Gabuniya, and Z. A. Kuteliya, "Tectonic Characteristics of the Caucasus," in *Geodynamics of the Caucasus* (Nauka, Moscow, 1989), pp. 3–15 [in Russian].
2. S. S. Arefiev, K. G. Pletnev, R. E. Tatevosyan, *et al.*, "Racha Earthquake of 1991: Results of In Situ Seismological Observations," Fiz. Zemli, No. 3, 12–23 (1993).
3. L. M. Balakina, "Focal Mechanisms of the Racha, April 29, 1991 Earthquake and Its Aftershocks in Relation to Their Geological Interpretation," Fiz. Zemli, No. 3, 42–52 (1993).
4. T. P. Belousov and V. P. Chichagov, "Coseismic Fractures and the Source Origin of the Racha Earthquake of 1991 in the Southern Greater Caucasus," Fiz. Zemli, No. 3, 53–63 (1993).
5. B. M. Bogachkin and E. A. Rogozhin, "Neotectonic Structure and Coseismic Deformations of the Epicentral Area of the Racha Earthquake," Geomorfologiya, No. 1, 57–72 (1993).
6. B. M. Bogachkin, Yu. V. Nechaev, E. A. Rogozhin, *et al.*, "Joint Analysis of Land-Based, Aerial, and Satellite Information in Relation to the Study of Epicentral Zones of Strong Earthquakes," Geomorfologiya, No. 4, 48–60 (1993).
7. B. A. Borisov, G. I. Reisner, and V. N. Sholpo, *Identification of Seismically Hazardous Zones in an Alpine Fold Area from Geological Data* (Nauka, Moscow, 1975) [in Russian].
8. D. Eberhart-Phillips, "Three-Dimensional Velocity Structure in Northern California Coast Ranges from Inversion of Local Earthquake Arrival Times," Bull. Seismol. Soc. Am. **76** (4), 1025–1052 (1986).
9. J. R. Evans, D. Eberhart-Phillips, and C. H. Thurber, "User's Manual for Simulps12 for Imaging V_p and V_p/V_s: A Derivative of the "Thurber Tomographic Inversion Simul3 for Local Earthquakes and Explosions," in *USGS, Open-File Report* (1994), pp. 94–431.
10. I. P. Gabsatarova, A. I. Zakharova, O. E. Starovoit, and L. S. Chepkunas, Preprint (Iaieine, 1992).
11. P. D. Gamkrealidze and I. P. Gamkrealidze, *Nappes of the Southern Slope of the Greater Caucasus* (Metsniereba, Tbilisi, 1977) [in Russian].
12. R. Gibson, K. Prentis, E. Fillip, *et al.*, "Ground Deformations Produced by the Racha Earthquake of April 29, 1991," in *Specification of Seismic Inputs (Problems of Engineering Seismology, Issue 34)* (Nauka, Moscow, 1993), pp. 123–136 [in Russian].
13. N. V. Kondorskaya, M. B. Mkrtchyan, and N. A. Lagova, "Analysis of the Spitak, December 7, 1988 Earthquake and Its Strong Aftershocks from Observations at Near Stationary and Teleseismic Stations," in *Comprehensive Assessment of Seismic Hazard (Problems of Engineering Seismology, Issue 32)* (Nauka, Moscow, 1991), pp. 25–35 [in Russian].
14. W. H. K. Lee and J. C. Lahr, "HYPO71 (Revised): A Computer Program for Determining Hypocenter, Magnitude and First Motion Pattern of Local Earthquakes," in *USGS, Open File Report, 75–311* (1975), pp. 75–311.
15. M. G. Leonov, *Wildflysch of Alpine Zones* (Nauka, Moscow, 1975) [in Russian].
16. E. E. Milanovsky, *Neotectonics of the Caucasus* (Nedra, Moscow, 1968) [in Russian].
17. E. E. Milanovsky and V. E. Khain, *Geological Structure of the Caucasus* (MGU, Moscow, 1963) [in Russian].
18. H. Philip, E. Rogozhin, A. Cisternas, *et al.*, "The Armenian Earthquake of December 7, 1988: Faulting and Folding Neotectonics and Paleoseismicity," Geophys. J. Int. **110**, 141–158 (1992).
19. M. T. Prilepin, S. Balasanyan, S. M. Baranova, *et al.*, "Kinematics of the Caucasian Region from GPS Data," Fiz. Zemli, No. 6, 68–75 (1997).
20. L. M. Rastsvetaev, "Lateral Faults and Alpine Geodynamics of the Caucasian Region," in *Geodynamics of the Caucasus* (Nauka, Moscow, 1989), pp. 106–113 [in Russian].
21. E. A. Rogozhin, L. N. Rybakov, and B. M. Bogachkin, "Seismic Deformations of the Earth's Surface Due to the Spitak Earthquake of 1988," Geomorfologiya, No. 3, 8–19 (1990).
22. E. A. Rogozhin, B. A. Borisov, and B. M. Bogachkin, "The Racha (Georgia) Earthquake of April 29, 1991: Data of Geological Inspection," Dokl. Akad. Nauk SSSR **321** (2), 353–358 (1991).

23. E. A. Rogozhin and B. M. Bogachkin, "Alpine and Recent Tectonics of the Racha Earthquake Area," Fiz. Zemli, No. 3, 3–11 (1993).

24. E. A. Rogozhin, S. S. Arefiev, B. M. Bogachkin, *et al.*, "Combined Analysis of Geological and Seismological Data and the Seismotectonic Reconstruction of the Racha Earthquake Source," Fiz. Zemli, No. 3, 70–77 (1993).

25. Yu. K. Shchukin, A. K. Astakhov, A. A. Belov, *et al.*, "Geological and Geophysical Conditions in the Source Zone of the Spitak Earthquake (on the 10th Anniversary of the Tragedy)," Geofizika, No. 5, 54–66 (1998).

26. N. V. Shebalin, *Strong Earthquakes (Selected Works)* (Akad. Gornykh Nauk, Moscow, 1997) [in Russian].

27. G. Sh. Shengelaya, *Gravity Model of the Caucasus Crust* (Nauka, Moscow, 1984) [in Russian].

28. C. H. Thurber, "Earthquake Locations and Three-Dimensional Crustal Structure in the Coyote Lake Area, Central California," J. Geophys. Res. **88** (B10), 8226–8236 (1983).

29. A. I. Zakharova, I. P. Gabsatarova, O. E. Starovoit, and L. S. Chepkunas, "Main Focal Parameters of the Racha Earthquake and Its Aftershocks," Fiz. Zemli, No. 3, 24–41 (1993).